

# Distribution and Textural Characterization of Tin in the Iska Iska Polymetallic Project, Bolivia

Natalia Goszczynski<sup>1\*</sup>, Lisa L. Van Loon<sup>1,3</sup>, Camila Aliaga-Morales<sup>1,2</sup>, Zohreh Ghorbani<sup>1</sup>, Osvaldo Arce-Burgoa<sup>2</sup>, William Pearson<sup>4</sup>, Neil R. Banerjee<sup>1</sup>

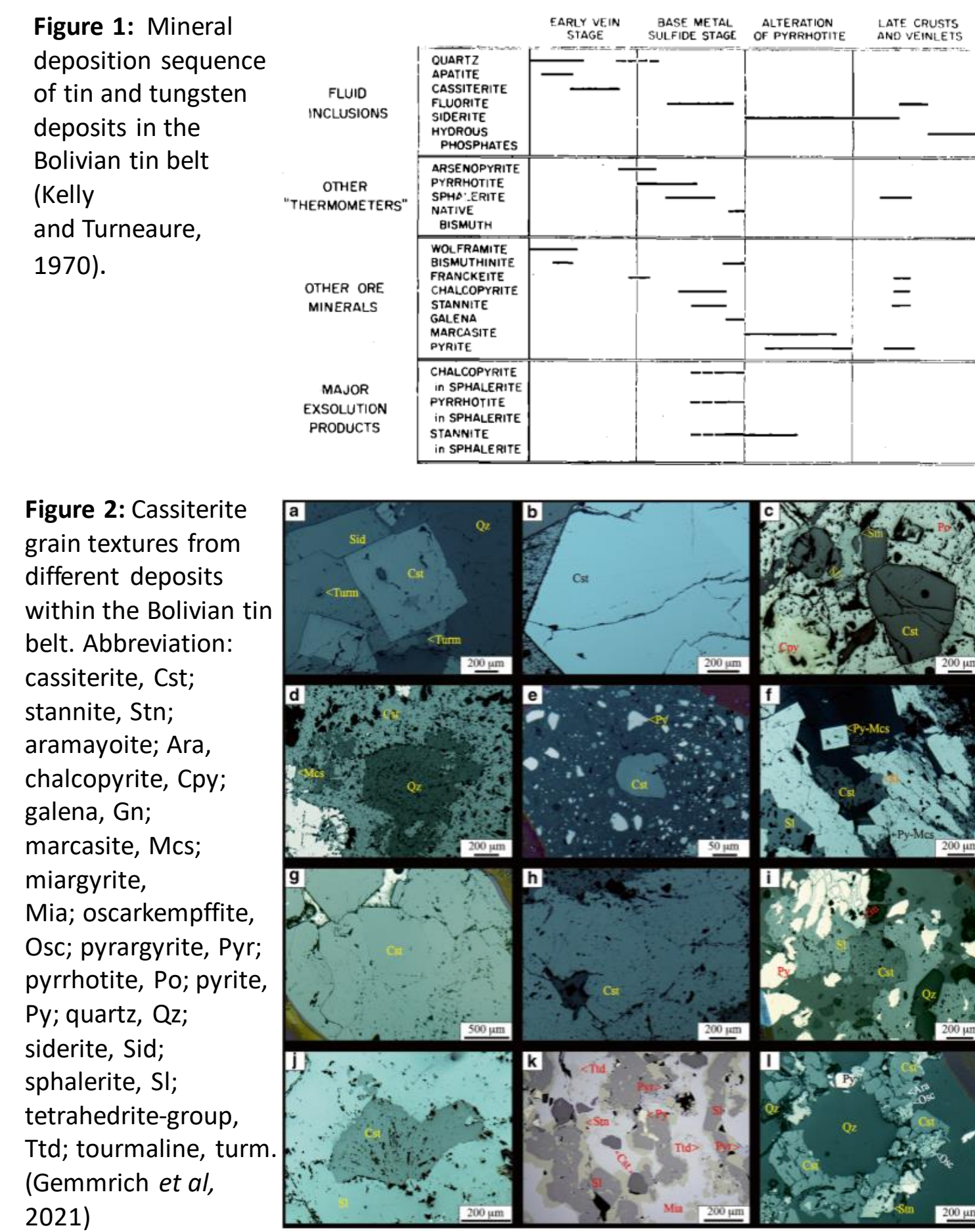


<sup>1</sup>Department of Earth Sciences, Western University, London, ON, Canada, <sup>2</sup>Minera Tupiza S.R.L. Eoro Resources Ltd., Sur Chichas Province, Potosi, Bolivia  
<sup>3</sup>LISA CAN Analytical Solutions INC, Saskatoon, Saskatchewan, Canada, <sup>4</sup>Eloro Resources Ltd., Toronto, Ontario, Canada  
 \*ngoszczy@uwo.ca



## Introduction

- The Iska Iska polymetallic project is located within the southern part of the Bolivian tin belt (BTB) and the Sud Chichas province of Bolivia
- The Iska Iska site consists of mainly Ag, Sn, Zn and Pb with a tin (W) porphyry style system at depth overprinted by an epithermal/xenothermal system near surface
- Cassiterite (SnO<sub>2</sub>) is the main tin mineral (Fig 2) found in the system and is thought to form in the early vein stage of mineralization with quartz, tourmaline and early pyrite at many of the deposits within the BTB (Fig 1) [1,4]
- Deposition temperatures of BTB cassiterite are between 300-500°C and 5-35wt% salinity from microthermometry [4,5]
  - Wood tin can form at temperatures as low as 150°C [3]
- Studies indicate that cassiterite is mainly transported in a chloride complex as Sn<sup>2+</sup> and deposited as Sn<sup>4+</sup> when the hydrothermal fluid increases in pH and oxygen fugacity while alkali chloride concentration decreases [2,3]
- Minimal research into textures, distribution styles, deposition environment and mineral association of tin minerals have been conducted in recent years within the BTB



## Tin Distribution and Textures

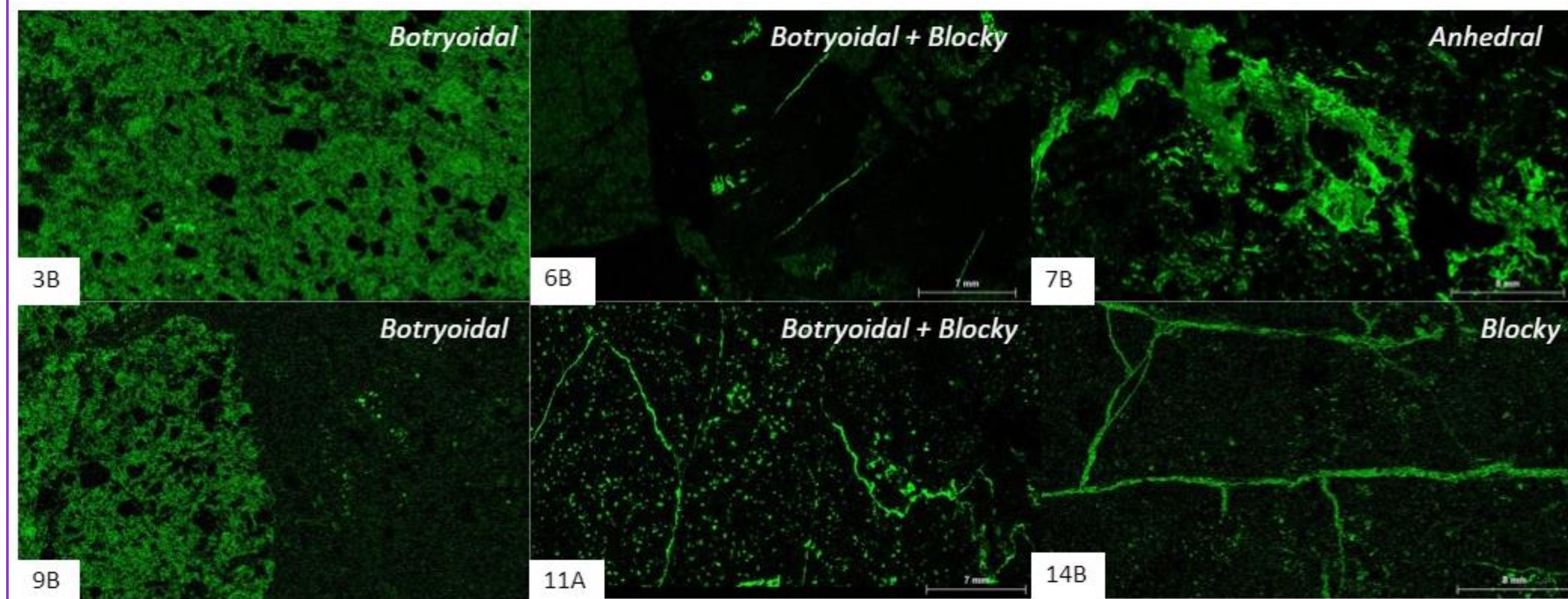


Figure 5: XRF tin maps of DSBU-3M samples. 3B: Dacite (at a depth of 77.16m) with interstitially distributed botryoidal tin. 6B: Pheatomagmatic breccia (at a depth of 195.80m) with narrow botryoidal high tin veins and clusters of blocky tin. 7B: Pheatomagmatic breccia (at a depth of 212.36m) with anhedral moderate to high tin, interstitial to disseminated distribution. 9B: Pheatomagmatic breccia (at a depth of 249.32m) with interstitial botryoidal moderate tin within fragments and minor botryoidal high tin clusters. 11A: Pheatomagmatic breccia (at a depth of 334.19m) with botryoidal high tin veins and disseminated blocky tin. 14B: Intrusion breccia (at a depth of 428.58m) with vein network of blocky tin.

- Main tin distribution styles observed in tin maps are **veining, interstitial and disseminated** (Fig 5)
- Common tin textures are **botryoidal, blocky and colloform** (Fig 5)
- Replacement textures of anhedral to subhedral cassiterite with anhedral galena and pyrite (Fig 6)
- Minor tetrahedrite, covellite and digenite associated with stannite in sample UWOSN-10 (Fig 7A)
- Based on EDS point analysis, only some cassiterite show small peaks of iron within grains and there is no zoning observed however petrography done on UWOSN samples show moderate to strong red hue of the grains normally caused by the presence of iron (Fig 7B)
- Fragmented cassiterite in pheatomagmatic breccia sample (Fig 7d)
- Colloform cassiterite commonly observed around quartz, pyrite, rutile grains and holes (Fig 8)

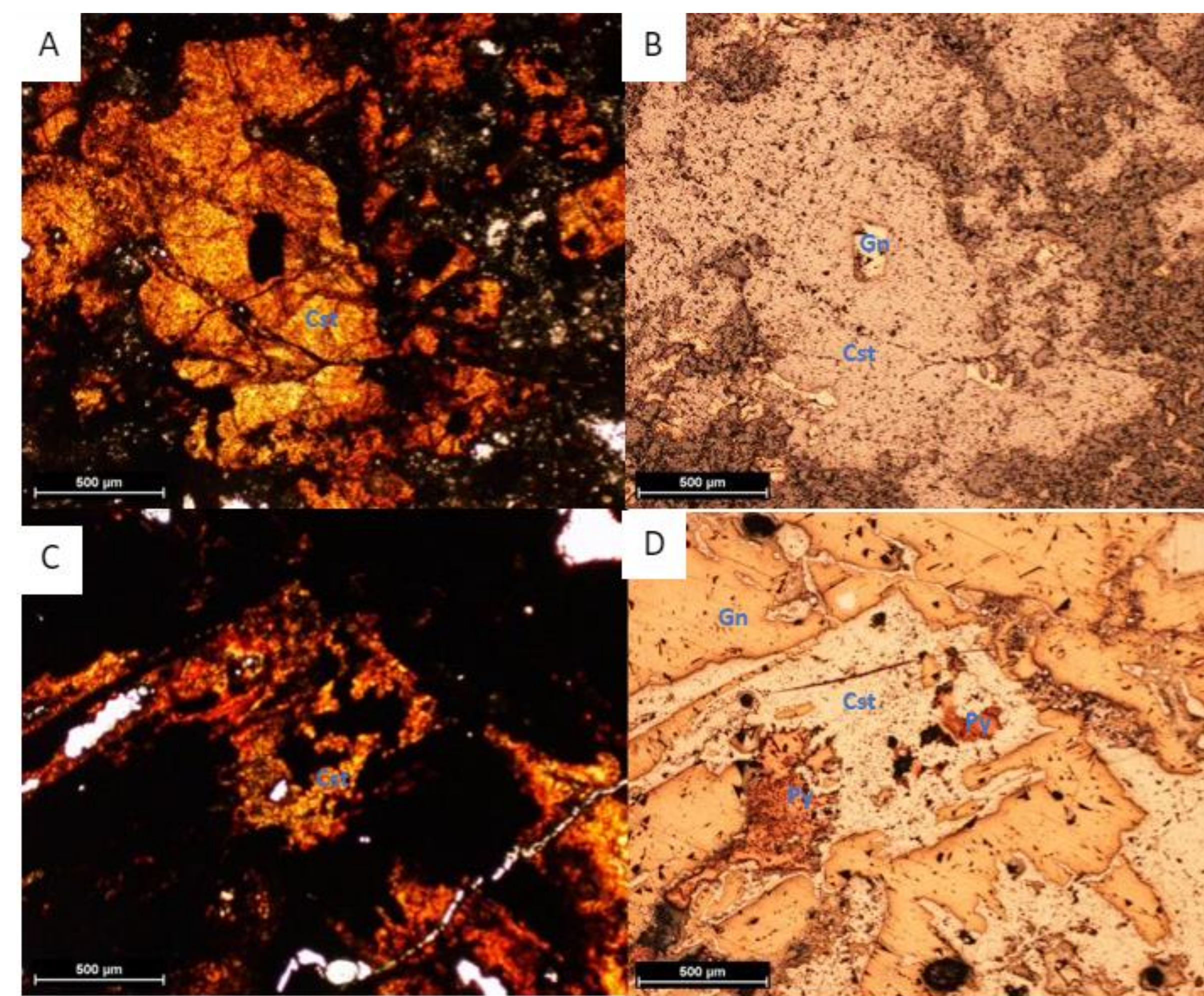


Figure 6: Photomicrographs of UWOSN samples with carbon coating. A: Transmitted ppl of sample UWOSN-02 (at a depth of 329.1m) showing anhedral fractures orange-yellow cassiterite with quartz matrix (Cst). B: Reflected ppl of sample UWOSN-02 (at a depth of 329.1m) showing anhedral galena (Gn) with sawtooth pitting partially replacing cassiterite (Cst). C: Transmitted ppl of sample UWOSN-08 (at a depth of 692.65m) showing anhedral red-orange cassiterite with a quartz vein and matrix (Cst). D: Reflected ppl of sample UWOSN-08 (at a depth of 692.65m) showing anhedral galena (Gn) with sawtooth pitting and pyrite (Py) replacing cassiterite (Cst).

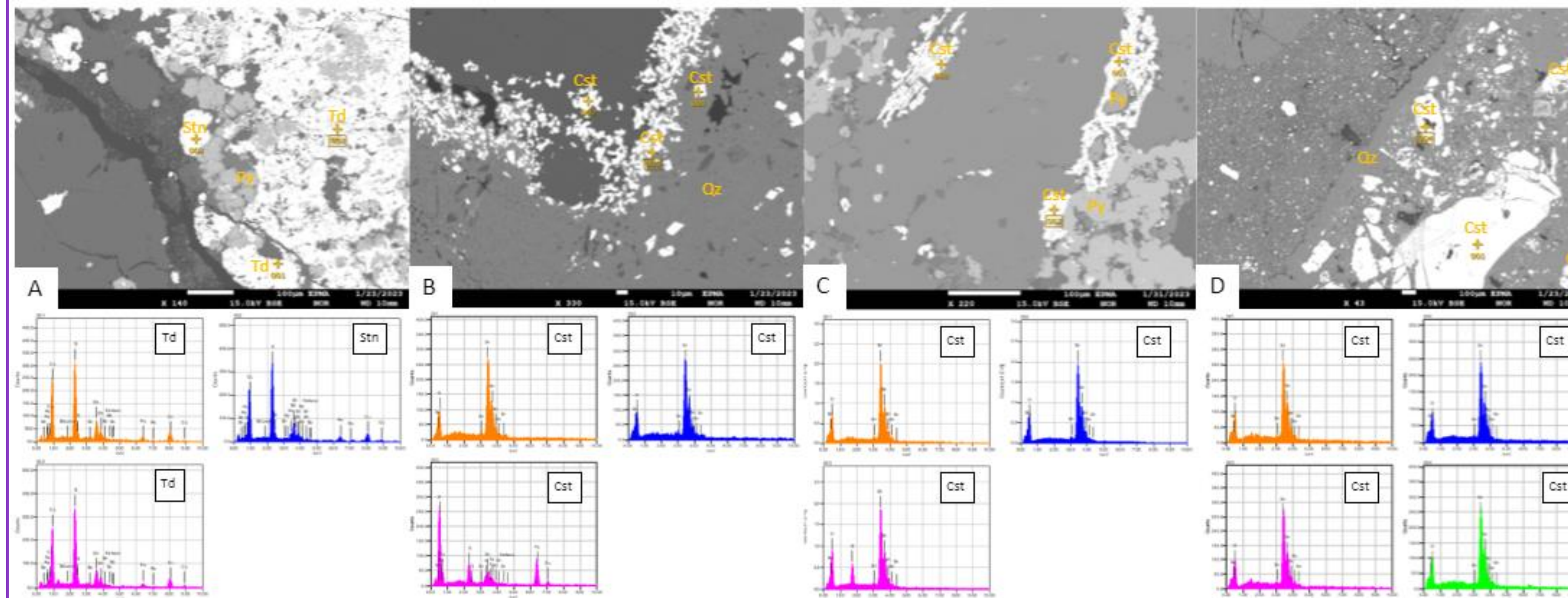


Figure 7: EDS images with corresponding EDS graphs of selected points below. A: Sample DSBU-3M-10 (at a depth of 298.05m) shows anhedral tetrahedrite and stannite replacing anhedral pyrite. B: Sample UWOSN-01 (at a depth of 98.87m) shows blocky euhedral cassiterite formed along the edge of a hole and a quartz grain. C: Sample DSBU-3M-7B (at a depth of 212.36m) shows elongated botryoidal cassiterite filling open space and formed around anhedral disseminated pyrite. D: Sample DSBU-3M-9B (at a depth of 362.74m) shows fragmented anhedral cassiterite with quartz crystals in pheatomagmatic breccia sample. Abbreviations: cassiterite, Cst; stannite, Stn; tetrahedrite, Td; quartz, Qz; pyrite, Py

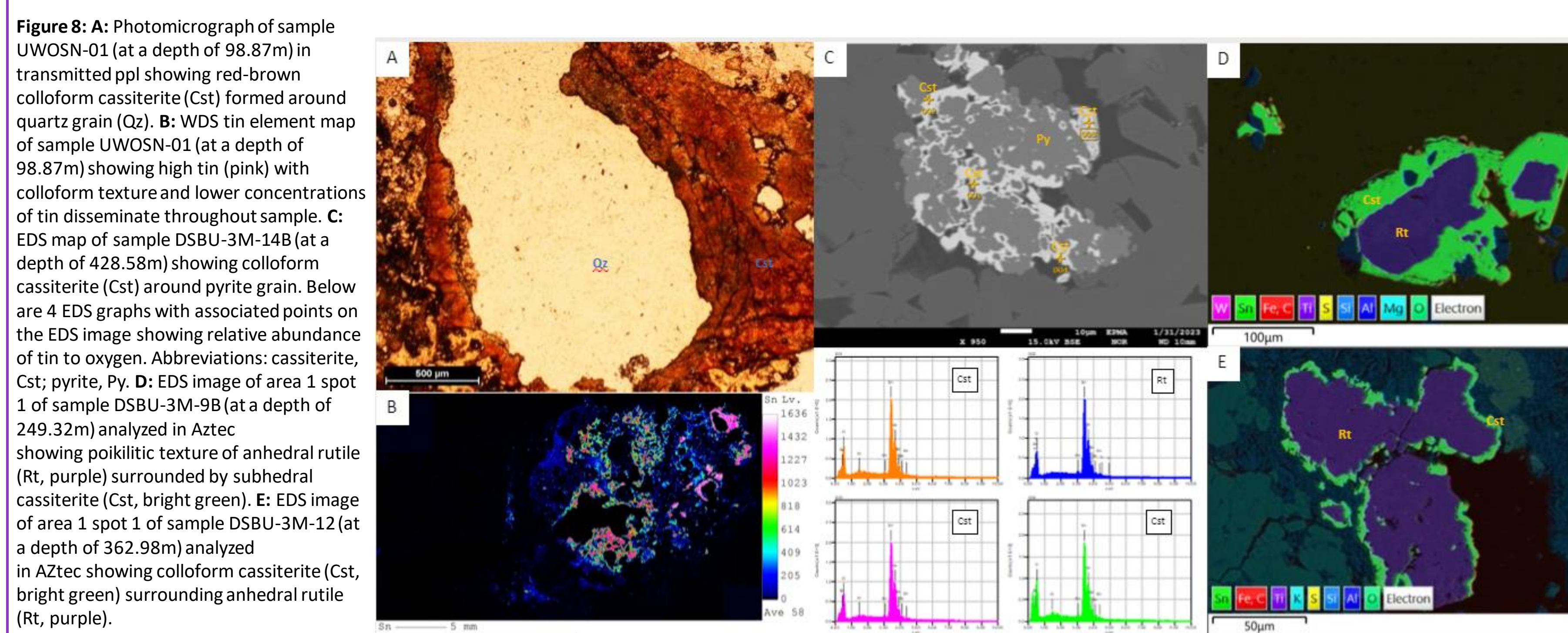


Figure 8: A: Photomicrograph of sample UWOSN-01 (at a depth of 98.87m) in transmitted ppl showing red-brown colloform cassiterite (Cst) formed around quartz grain (Qz). B: WDS tin element map of sample UWOSN-01 (at a depth of 98.87m) showing high tin (pink) with colloform texture and lower concentrations of tin disseminate throughout sample. C: EDS map of sample DSBU-3M-14B (at a depth of 428.58m) showing colloform cassiterite (Cst) around pyrite grain. Below are 4 EDS graphs with associated points on the EDS image showing relative abundance of tin to oxygen. Abbreviations: cassiterite, Cst; pyrite, Py. D: EDS image of area 1 spot 1 of sample DSBU-3M-9B (at a depth of 249.32m) analyzed in AZtec showing colloform cassiterite (Cst, bright green) surrounding anhedral rutile (Rt, purple).

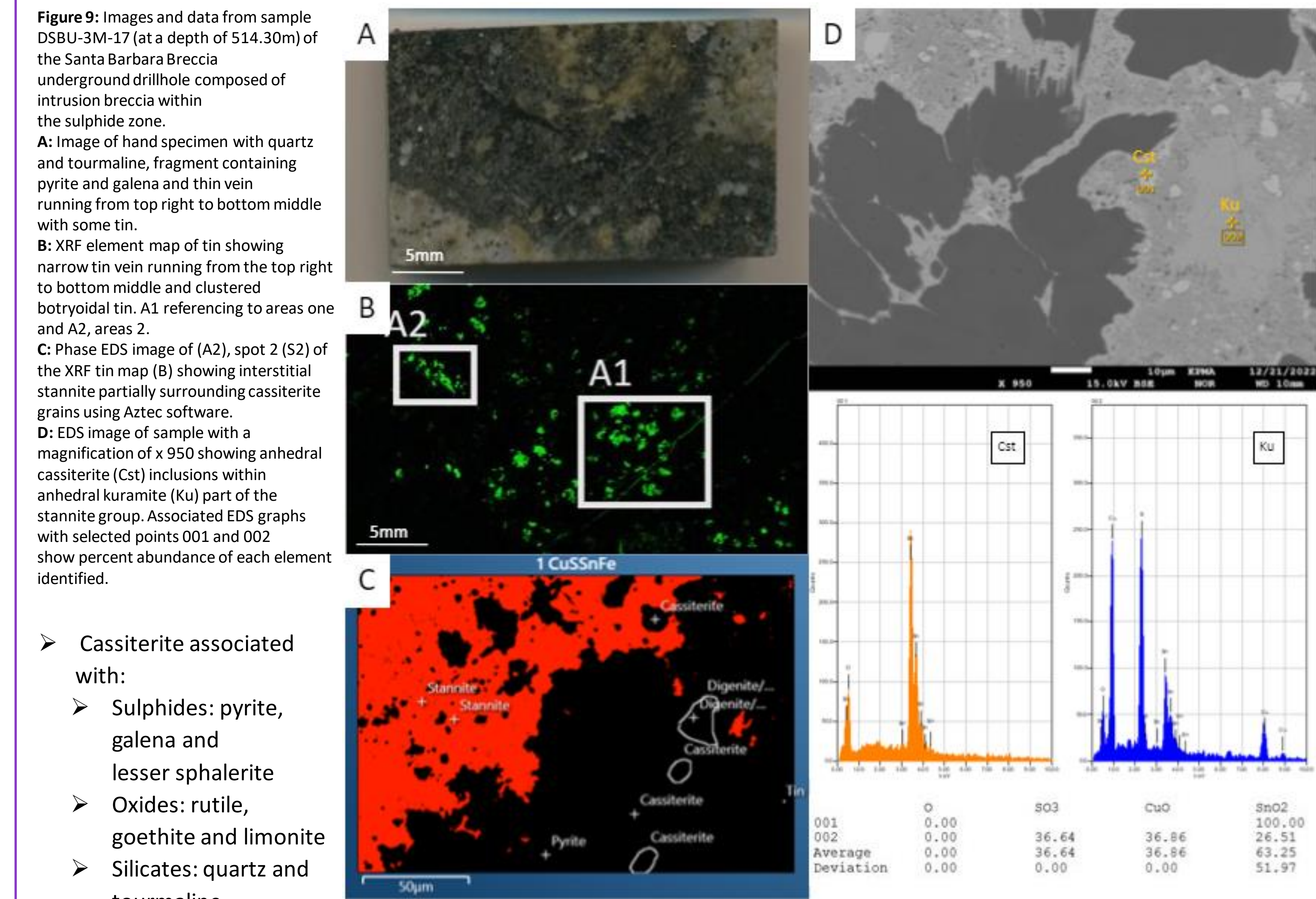


Figure 9: Images and data from sample DSBU-3M-17 (at a depth of 514.30m) of the Santa Barbara Breccia underground drillhole composed of intrusion breccia within the sulphide zone. A: Image of hand specimen with quartz and tourmaline, fragment containing pyrite and galena and thin vein running from top right to bottom middle with some tin. B: XRF element map of tin showing narrow tin vein running from the top right to bottom middle and clustered botryoidal tin. A1 referencing to areas one and A2, areas 2. C: Phase EDS image of (A2), spot 2 (S2) of the XRF tin map (B) showing interstitial stannite partially surrounding cassiterite grains using Atece software. D: EDS image of sample with a magnification of x950 showing anhedral cassiterite (Cst) inclusions within anhedral kuramite (Ku) part of the stannite group. Associated EDS graphs with selected points 001 and 002 show percent abundance of each element identified.

- Cassiterite associated with:
  - Sulphides: pyrite, galena and lesser sphalerite
  - Oxides: rutile, goethite and limonite
  - Silicates: quartz and tourmaline
- From hand specimens and core log date cassiterite is difficult to identify with the unaided eye, even with tin abundances of up to 22% (Fig 9a)
- Sample DSBU-3M-17 exhibited cassiterite inclusions within kuramite (Cu<sub>2</sub>SnS<sub>4</sub>) part of the stannite group (Fig 9D)
  - Anhedral stannite (Cu<sub>2</sub>FeSn<sub>4</sub>) identified with interstitial and disseminated textures using EDS images and maps (Fig 9C)
- Tin percent range for sample suite DSBU-3M is 0.085-4.1% and UWOSN is 0.2-22.72%, using handheld microprobe

## Discussion

- Based on EDS images and graphs stannite group minerals and tetrahedrite formed after cassiterite where they surrounded the small cassiterite grains during a reducing hydrothermal fluid phase
- The association of iron bearing oxide minerals with high tin grade samples and the red hue of grains (UWOSN) suggest possible presence of wood tin that can form at low temperatures (from 150°C) however petrography on cassiterite zoning was inconclusive
- Cassiterite deposited around the same time or shortly after quartz, tourmaline and early pyrite since there is some cassiterite that forms around quartz and replaces pyrite
  - Late pyrite, galena and sphalerite formed after cassiterite because of replacement textures, indicating initial oxidizing hydrothermal fluid phase followed by reducing fluid phase
- Fragmented and fractured cassiterite in breccia may indicate brecciation event after deposition therefore after the early vein stage of mineralization
- Blocky and botryoidal textures may indicate early deposition of cassiterite because their euhedral shape and large size whereas interstitial and anhedral textures could represent late-stage deposition due to reduced time and available space to grow

## Conclusion and Future Implication

- High tin concentration in cassiterite found mainly distributed as disseminated, interstitial or as veins with botryoidal, colloform and blocky textures
  - Distribution styles and textures can be used as indicators for moderate to high tin within the project
  - By better understanding the textures and elements associated with the tin more efficient refining process can be achieved for greater recovery
- Since cassiterite is hard to identify in core logging; assays of tin, petrography and or EDS data will have to be used to more accurately identify the amount of tin present
- Data should be collected using microthermometry to determine the depositional temperature and fluid salinity of cassiterite fluid inclusions in the system
- Paragenetic sequence of the system should be developed
- Research into the magma intrusion (granodiorite) composition should be conducted to evaluate the source and origin of tin in the system
- Cathodoluminescence studies to confirm presence of cassiterite zoning in the system (wood tin)

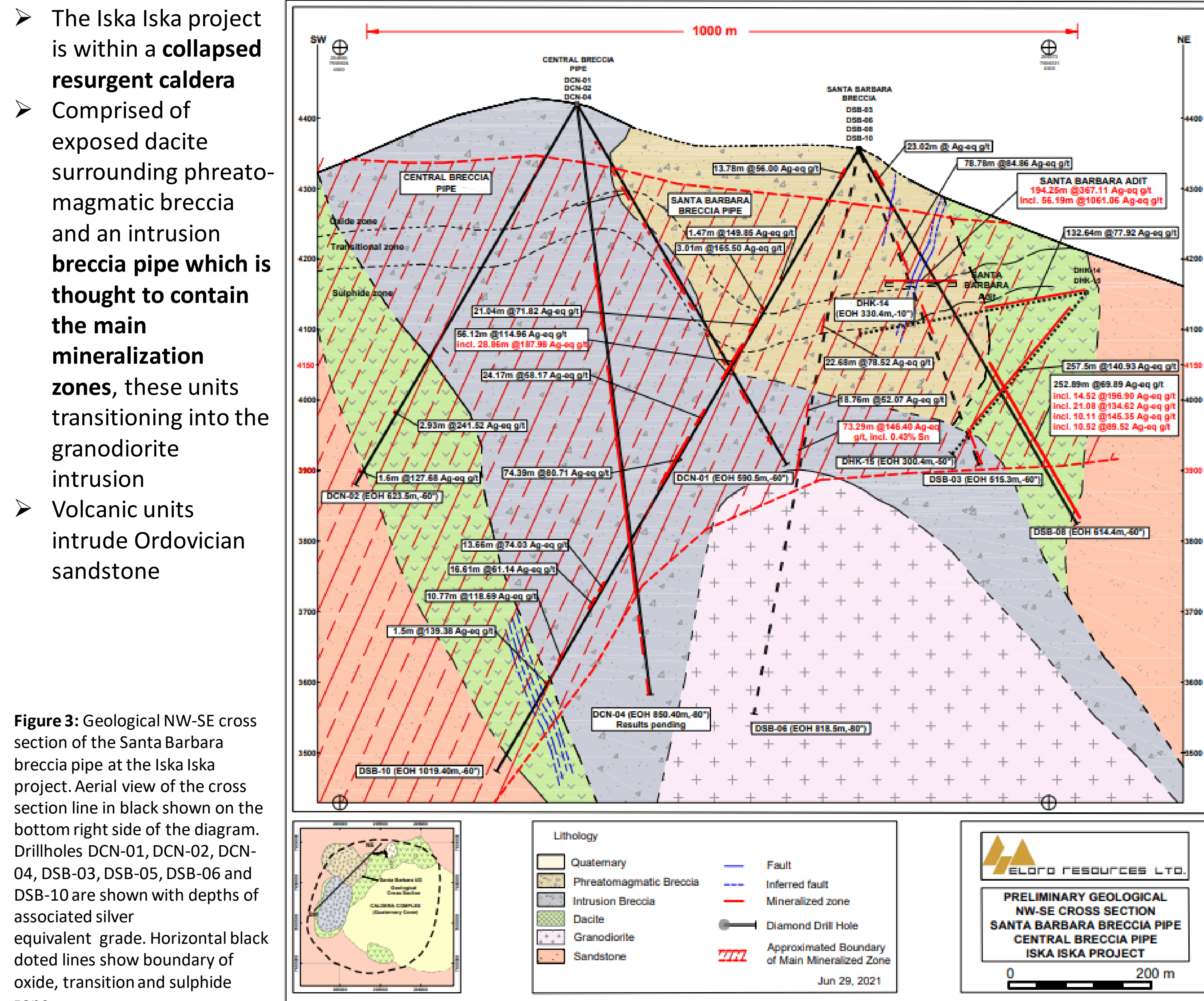
## Acknowledgment

Thank you to Eloro Resources Ltd for allowing us access to the project site, drillhole data and collect samples, as well as the University of New Brunswick for their XRF and SEM work.

## References

- Gemrich, L., Torró, L., Melgarejo, J. C., Laurent, O., Vallance, J., Chelle-Michou, C., & Sempere, T. P. (2021). Trace element composition and U-Pb ages of Cassiterite from the Bolivian Tin Belt. *Mineralium Deposita*, 56(8), 1491–1520.
- Heinrich, C. A. (1990). The chemistry of hydrothermal tin(-tungsten) ore deposition. *Economic Geology*, 85(3), 457–481.
- Inverno, C. M., & Hutchinson, R. W. (2004). The endogranitic tin zone, Mount Pleasant, New Brunswick, Canada and its metallogensis. *Applied Earth Science*, 113(4), 261–288.
- Kelly, W. C., & Turneure, F. S. (1970). Mineralogy, paragenesis and geothermometry of the tin and tungsten deposits of the Eastern Andes, Bolivia. *Economic Geology*, 65(6), 609–680.
- Lehmann, B. (2021). Formation of tin ore deposits: A reassessment. *Lithos*, 402–403, 105756.

## Geology of Iska Iska



## Methodology

- One sample suite was collected from different depth intervals of a single drillhole and the second suite collected samples with high tin grade from multiple drillholes with varying composition
- X-ray fluorescence (XRF) elemental maps of Sn, Fe, S, Pb, Cu, Sr and Si of one sample suite were made at the University of New Brunswick along with energy dispersive spectroscopy (EDS) and back scatter electron (BSE) maps of high tin concentration areas within selected samples
  - Areas were then subdivided into two or three spots and analyzed in AZtec software for mineral phases
- Wave dispersive spectroscopy (WDS) was used to obtain tin element maps of the second sample suite
- Samples with abundant tin, different distribution styles and varying minerals associated with cassiterite were selected for point analysis using the electron probe micro-analyzer (EPMA)
- Petrography was conducted on all 37 samples

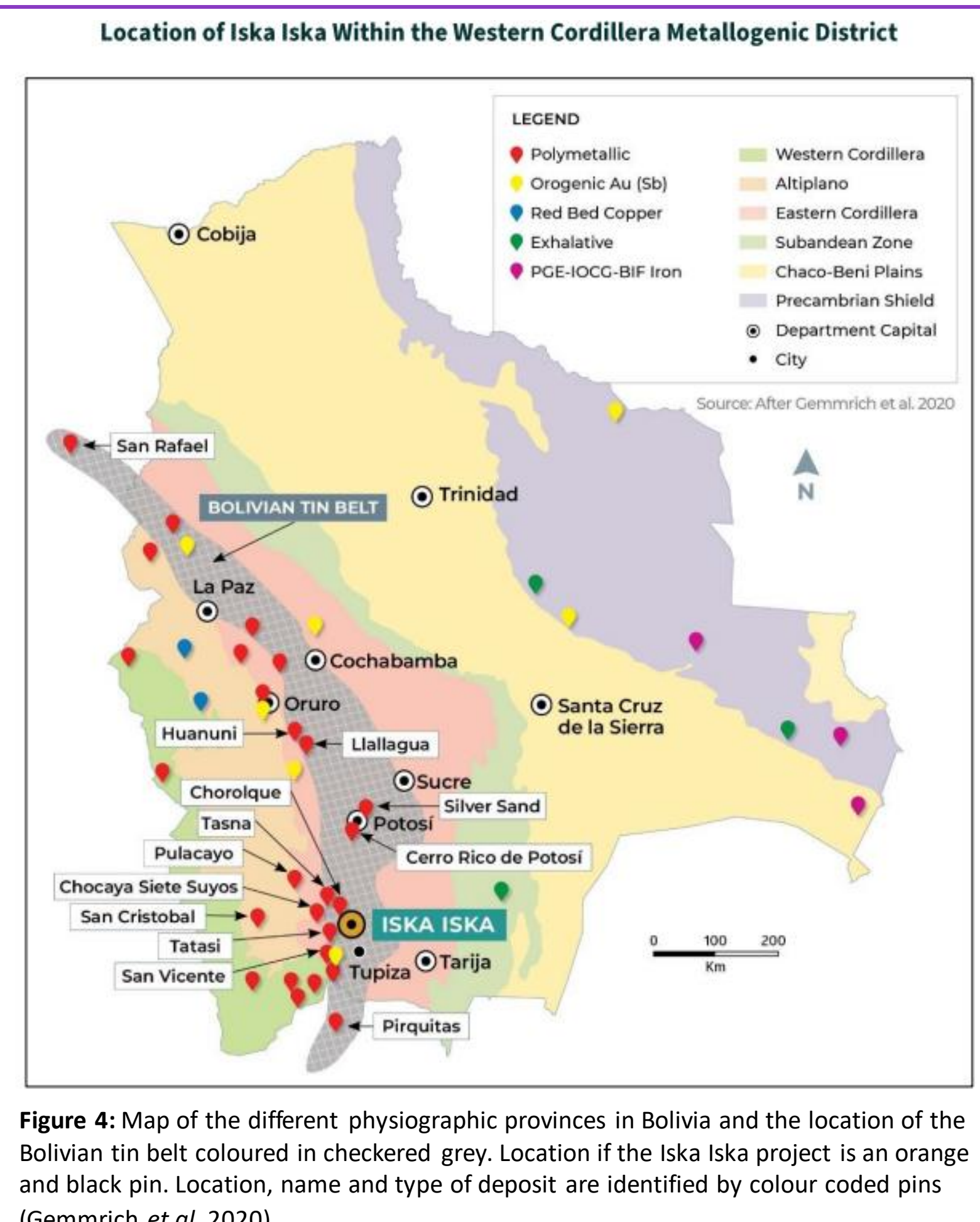


Figure 4: Map of the different physiographic provinces in Bolivia and the location of the Iska Iska project. Location of the Iska Iska project is an orange and black pin. Location, name and type of deposit are identified by colour coded pins (Gemrich et al., 2020).